IEEE Access
Multidisciplinary | Rapid Review | Open Access Journal

Received February 18, 2020, accepted March 8, 2020, date of publication March 16, 2020, date of current version March 26, 2020.

Digital Object Identifier 10.1109/ACCESS.2020.2981015

A Novel Hybrid Fusion Algorithm for Low-Cost GPS/INS Integrated Navigation System During GPS Outages

DENGAO LI[1,2], XUAN JIA[2,3], AND JUMIN ZHAO[2,3]
[1]College of Data Science, Taiyuan University of Technology, Jinzhong 030600, China
[2]Shanxi Engineering Technology Research Center for Spatial Information Network, Jinzhong 030600, China
[3]College of Information and Computer, Taiyuan University of Technology, Jinzhong 030600, China

Corresponding author: Dengao Li (lidengao@tyut.edu.cn)

The work was supported in part by the General Object of National Natural Science Foundation under Grant 61772358: Research on the key technology of BeiDou Navigation Satellite System precision positioning in complex landform, in part by the General Object of National Natural Science Foundation under Grant 61972273: Research on Adaptive Modulation Theory and Key Technologies for Passive Sensor Systems, in part by the International Cooperation Project of Shanxi Province under Grant 201603D421012 : Research on the key technology of Global Navigation Satellite System area strengthen information extraction based on crowd sensing, in part by the Transformation and Cultivation Project of Scientific and Technological Achievements of Universities in Shanxi Province: Disaster early warning system based on BeiDou Navigation Satellite System high-precision positioning technology, and in part by the National Key Research and Development Project under Grant 2018YFB2200900 Broadband Optical Transceiver Integrated Devices and Modules for Data Center Applications.

ABSTRACT It is the main challenge for Global Positioning System (GPS)/Inertial Navigation System (INS) to achieve reliable and low-cost positioning solutions during GPS outages. A new GPS/INS hybrid method is proposed to bridge GPS outages. Firstly, a data pre-processing algorithm based on empirical mode decomposition (EMD) for wavelet de-noising is developed to reduce the uncertain noise of IMU raw measurements and provide accurate information for subsequent GPS/INS data fusion and training samples. Then, the interactive multi-model extended Kalman filter(IMM-EKF) algorithm is proposed to improve the robustness of Kalman filter output and the accuracy of model training target output. Finally, a new intelligent structure of GPS/INS based on Extreme Learning Machine (ELM) is proposed. When the GPS is available, the IMM-EKF is used to fuse the GPS and de-noised INS data, and the de-noised INS data and the outputs of IMM-EKF are used to train the ELM. During GPS outages, the ELM is used to predict and correct the INS position error. In order to evaluate the effectiveness of the proposed method, 3 tests were performed in the actual field test. The comparison results show that the proposed fusion method can significantly improve the accuracy and reliability of positioning during GPS outages.

INDEX TERMS Inertial navigation system, GPS outages, data fusion, position error.

I. INTRODUCTION

Global Positioning System (GPS) and Inertial Navigation System (INS) are the two most commonly used positioning systems today [1]. GPS can provide accurate position and velocity information when it has direct line of sight with at least four satellites [2]. However, it is unstable due to the number of accessible satellites, multipath effects and external environment [3]. INS uses three accelerometers and three gyroscopes to provide dynamic measurements of high-frequency updates in a short period of time, but due to drift effects, measurement errors will accumulate [4]. In order to combine the advantages and make up for those shortcomings, GPS/INS integrated navigation has been widely used in dynamic navigation and positioning [5].

In general, GPS/INS integrated navigation uses a Kalman filter (KF) for information fusion [6]. GPS measurement signals can be optimally estimated for inertial navigation system errors and feed back to the inertial navigation system for error correction. Extended Kalman Filter (EKF), as an extension of KF, has been widely used in GPS and INS integration to provide a robust navigation solution [7]. However, the Kalman filtering algorithm requires that the process noise covariance and the measurement noise covariance are accurately known in prior knowledge [8]. Inaccurate knowledge of process noise and measurement noise will result in the reduction of positioning performance [9]. In the actual environment, GPS signal is easily blocked, so the GPS cannot

The associate editor coordinating the review of this manuscript and approving it for publication was Ehsan Asadi.

output the measurement information, and the filtering method will be ineffective. The error of the inertial navigation system will accumulate over time, which will cause the navigation information to diverge.

For high-grade INS, accurate positioning information can also be output independently during GPS outages [10]. However, high-grade INS cannot be widely used because of the high cost. Recently, micro-electromechanical systems (MEMS) INS have been widely used in GPS/INS integration because of their low cost [11]. Compared to high-grade INS, low-cost INS have large sensor errors, and their measurements have high noise, bias and drift errors. During GPS outage, GPS/INS integrated navigation was forced into pure INS mode and the INS errors could not be corrected by Kalman outputs [12]. Due to the large random errors, the positioning accuracy of the low-cost INS is rapidly reduced in a short time, which cannot meet the requirements of positioning and navigation [13].

In recent years, many methods have been proposed to improve positioning accuracy of GPS/INS during GPS outages [14]. There are several common artificial intelligence (AI) methods, such as Back Propagation Neural Network (BPNN) [15], Multi-Layer Perceptron (MLP) [16], Radial Basis Function Neural Networks (RBFNN) [17], Random Forest Regression (RFR) [18] and Support Vector Machine (SVM) [18]. The AI-based methods relate INS errors at a certain time instant to the corresponding INS outputs at the same instant. In order to address the dependence of the INS errors, an input-delay neural network (IDNN) was proposed to simulate INS position errors based on current and past samples of INS position, and it demonstrates better performance during GPS outages [19].

When these methods based on neural network are applied to low-cost GPS/INS, the basic idea is to collect INS data and Kalman filter outputs as training samples to train the neural network model when the GPS is available. During GPS outages, the outputs of Kalman filter are predicted by neural network to correct the INS errors [20]. However, all these methods assume that neural networks are trained under ideal conditions, without considering the accuracy of the training samples. Specifically, on the one hand, the IMU raw measurement data has complex noise characteristics. These methods do not take into account the uncertain noise in the raw data of the inertial sensor [21]. They all lack proper and efficient pre-processing algorithm to mitigate uncertain noise in the raw measurements of inertial sensors before data fusion. On the other hand, the reliability of the Kalman filtering results as the predicted target outputs are not considered. Considering that GPS is susceptible to dilution of low altitude accuracy and multipath effect, the positioning performance will also decrease. These GPS measurement errors will lead to random measurement noise and increased uncertainty in the statistical properties of the measurement noise,which will result in degradation or even divergence of the Kalman filter results [22]. The uncertainty of these training samples increases the complexity of the nonlinear input/output relationship model, which limits the prediction accuracy [23].

The complexity of noise in the actual environment and the variability of target motion will lead to large estimation errors in positioning information [6]. In order to obtain reliable and accurate positioning information during GPS outages, a novel hybrid fusion algorithm is proposed to bridge GPS outages.

Firstly, a data pre-processing algorithm based on empirical mode decomposition (EMD) for wavelet de-noising is developed to process IMU raw measurements and improve the accuracy of training inputs. The low-cost INS raw measurements are mixed with a lot of noise, and the wavelet de-noising algorithm is not ideal [24]. The EMD-based filtering algorithm will remove the useful signal on the corresponding component, which causes severe distortion of the signal [25]. The proposed algorithm can increase the signal-to-noise ratio and provide accurate information for subsequent GPS/INS data fusion and model training inputs.

Secondly, the EKF algorithm requires the measurement noise covariance to be accurately known in the prior. However, the actual measurement noise covariance is dynamically changed [26]. Therefore, the interactive multi-model (IMM) algorithm is introduced into EKF, which is called IMM-EKF, to implement dynamic interaction and dynamic changes of different measurement noise covariances. The proposed algorithm can improve the robustness of Kalman filter outputs and the accuracy of model training target outputs.

Finally, an extreme learning machine (ELM) is proposed to improve the prediction performance during GPS outages. The IMU raw measurements and Kalman outputs are processed separately by the above two methods to obtain accurate training samples. Then, the new intelligent structure of GPS/INS based on ELM is proposed to bridge GPS outages. The feature of ELM is simple structure, fast learning, good global search performance and generalization performance,which can improve predictive performance during GPS outages [27].

The structure of the paper is organized as follows. Section 2 introduces the training model and the predicting model of the proposed GPS/INS fusion algorithm in detail. Section 3 proposes the wavelet de-noising method based on EMD to process IMU raw measurements. Section 4 introduces the GPS/INS algorithm based on IMM-EKF when the GPS is available. Section 5 introduces the principles and training methods of GPS/INS integrated navigation based on ELM. Section 6 introduces and discusses the road experimental tests to verify the proposed hybrid method. Finally, section 7 draws the conclusions.

II. GPS/INS MODEL DESCRIPTION

The proposed GPS/INS fusion algorithm includes a training phase and a prediction phase. Fig. 1 shows the training mode of limiting INS error growth by filtering output when the GPS is available. MEMS-IMU consists of three-axis accelerometers and three-axis gyroscopes. w_x, w_y, w_z are the

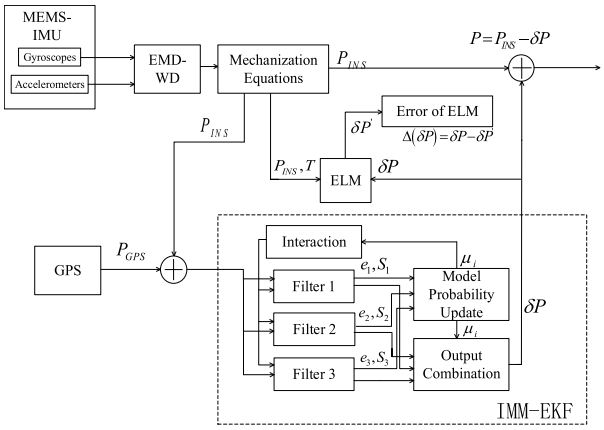

FIGURE 1. The block diagram of training phase.

gyroscope outputs in X, Y, and Z directions. a_x, a_y, a_z are the acceleration outputs by the accelerometer in X, Y, and Z directions, respectively. In Fig. 1, EMD-WD refers to the wavelet de-noising algorithm based on EMD. Its inputs are IMU raw measurements, which include w_x, w_y, w_z and a_x, a_y, a_z. Its outputs are the de-noised IMU measurements. Fig. 3 is the block diagram of EMD-WD. The inputs of the mechanization equation are the de-noised IMU measurements, and the output is the INS position P_{INS}. In Fig. 1, the outputs of INS and GPS are P_{INS} and P_{GPS}, respectively. Then, the residual of the position information of the two is used as the observation of the IMM-EKF fusion algorithm. Then, the output δP of IMM-EKF is used to correct the position information P_{INS}. As shown in the dotted box in Fig. 1, the IMM-EKF is set to three filter models. The difference between the three filter models is the difference in covariance matrix of the noise model. The algorithm consists of four steps and the specific process is detailed in section 4. The training inputs of ELM are P_{INS} and time T. The training target output is filter output δP of IMM-EKF. The actual training output is $\delta P'$. $\Delta(\delta P)$ is the difference between the two. It represents the ELM prediction error.

$$\Delta(\delta P) = \delta P' - \delta P \tag{1}$$

Then, the output position when the GPS is available is:

$$P = P_{INS} - \delta P \tag{2}$$

Fig. 2 shows the prediction model for correcting INS position errors during GPS outages. During GPS outages, the EMD-WD is used to pre-process the IMU raw measurements. Fig. 3 is the block diagram of EMD-WD. The inputs of the mechanization equation are the de-noised IMU measurements, and the output is the INS position P_{INS}. During GPS outages, P_{INS} and T input into ELM and ELM is used to predict the output $\delta P'$ of IMM-EKF. In other words, the predicted output of IMM-EKF is the predicted INS position errors.

During GPS outages, the latest learning rule base before GPS outages is used to switch the system to the prediction

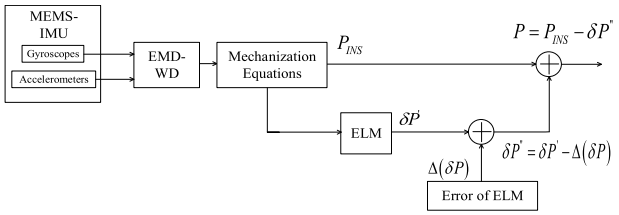

FIGURE 2. The block diagram of predicting phase.

mode and predict the INS positioning error. In Fig. 2, $\delta P''$ is the filter output of ELM prediction.

$$\delta P'' = \delta P' - \Delta(\delta P) \tag{3}$$

Then, the output position during GPS outages is:

$$P = P_{INS} - \delta P'' \tag{4}$$

III. DATA PRE-PROCESSING ALGORITHM

A. WAVELET DE-NOISING

The basic idea of wavelet transform approximates the original function with a family of wavelet bases. Through wavelet transform, the signal is decomposed into multi-scale wavelet coefficients arranged according to the frequency, i.e. wavelet decomposition components. The main idea of wavelet de-noising is to set a threshold. The high frequency coefficients are threshold processed. Then, the signal is reconstructed to eliminate the effects of noise. The threshold function includes a soft threshold function and a hard threshold function.

The hard threshold function is:

$$\hat{d} = \begin{cases} d, & |d| \geq \lambda \\ 0, & |d| < \lambda \end{cases} \tag{5}$$

The soft threshold function is:

$$\hat{d} = \begin{cases} \mathrm{sgn}(d)(|d| - \lambda), & |d| \geq \lambda \\ 0, & |d| < \lambda \end{cases} \tag{6}$$

where, d is the unprocessed wavelet coefficient, and $\hat{d}$ is the wavelet coefficient after the threshold processing, λ is the set threshold.

$$\mathrm{sgn}(x) = \begin{cases} 1, & ,x > 0 \\ 0, & x = 0 \\ -1, & x < 0 \end{cases} \tag{7}$$

To implement the wavelet filter, wavelet function "db6" with soft thresholding scheme based on Stein's Unbiased Risk Estimate (SURE) is adopted. It is an unbiased estimate of the mean square error criterion and it tends to an ideal threshold. The threshold λ is:

$$\lambda = \arg\min_{T>0} \left\{ \left[\sum_{i=0}^{N} (|d_i| \wedge \lambda)^2 + N\sigma_n^2 - 2\sigma_n^2 \sum_{i=0}^{N} I(|d_i| < \lambda) \right] \right\} \tag{8}$$

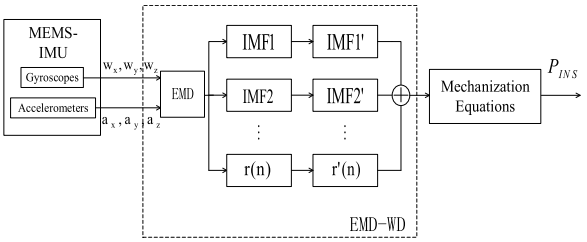

FIGURE 3. The block diagram of EMD-WD.

In which arg {min f(λ)} represents the λ value when f(λ) is minimized. The symbol ∧ indicates taking the minimum of the two numbers. σ_n^2 represents the noise standard deviation.

$$I(x) = \begin{cases} 1, & true \\ 0, & false \end{cases} \tag{9}$$

B. WAVELET DE-NOISING BASED ON EMD

Based on the original wavelet threshold de-noising, the data pre-processing algorithm based on empirical mode decomposition (EMD) for wavelet de-noising is developed to process IMU raw measurements and improve the accuracy of training inputs for ELM. The EMD method is an important part of the Hilbert-Huang Transform. It decompose the signal into several Intrinsic Mode Functions (IMFs), which contain different time scales. When IMF component $c_n(t)$ or residual signal $r_n(t)$ is less than the preset value, or $r_n(t)$ is a monotone function, the whole screening process ends. After the above steps, it can be decomposed into the sum of n IMF components and residual signal.

$$x(t) = \sum_{i=1}^{n} c_i(t) + r_n(t) \tag{10}$$

The low-cost INS raw measurements are mixed with a lot of noise. Considering that the noise is decomposed and distributed on each IMF component, all IMF components can be processed in combination with the wavelet de-noising method. EMD-WD is proposed to pre-process the IMU raw measurements. Its inputs are IMU raw measurements and outputs are the de-noised IMU measurements. In order to facilitate writing, the MEMS-IMU raw measurements which include the gyroscope outputs a_x, a_y, a_z and the gyroscope outputs w_x, w_y, w_z are represented as the signal $x(t)$. Fig. 3 is the block diagram of EMD-WD.

The proposed data pre-processing algorithm steps are:

1)Signal $x(t)$ is decomposed by EMD to obtain each IMF component;

2)Each IMF component performs wavelet threshold de-noising to obtain de-noised IMF component;

3)The signal is reconstructed by the de-noised IMF components.

$$x'(t) = \sum_{i=1}^{n} c_i'(t) + r_n'(t) \tag{11}$$

where, $x'(t)$ is the de-noised signal, $c_i'(t)\ (i = 1, 2, \ldots, n)$ and $r_n'(t)$ are the de-noised IMF components.

After EMD-WD, the mechanization equation can output the de-noised INS data.

IV. INTERACTIVE MULTI-MODEL KALMAN FILTER ALGORITHM

As shown in Fig.1. The outputs of Kalman filter algorithm are the training target outputs of ELM. Therefore, the robustness of the Kalman filter algorithm must be considered in the practical environment. IMM-EKF is proposed to improve the robustness of Kalman filter outputs and the accuracy of model training target outputs.

A. KALMAN FILTER ALGORITHM

The KF is a basic and practical data fusion method widely used in GPS/INS. The process model and measurement model of KF are:

$$\begin{cases} x = Fx + Gw \\ z = Hx + v \end{cases} \tag{12}$$

where, v is measurement noise vectors and R is measurement noise covariance matrix. The KF algorithm assumes that the GPS output error model is a white noise with a zero-mean Gaussian distribution of known statistical properties. In other words, the measurement noise covariance matrix R is fixed throughout the KF process. In the actual environment, the size of the GPS output error model changes. Once the assumed measurement noise covariance cannot match the measurement noise of the actual process, the effect of the Kalman filter fusion output is less than ideal, and the adaptability is relatively poor.

B. INTERACTIVE MULTI-MODEL EXTENDED KALMAN FILTER ALGORITHM

The principle of IMM is to design multiple measurement noise covariances according to different working states of the system. These models can adjust the probability of each model in real time, and use Markov chain and likelihood function to adjust the mutual conversion between models in real time, which can better match the actual situation of the system.

IMM-EKF is proposed to implement dynamic interaction and dynamic changes of different measurement noise covariances. The proposed IMM-EKF algorithm can improve the robustness of Kalman filter outputs and the accuracy of training target outputs. A model set is designed, which has different zero mean Gaussian distributions and different covariance matrices. The covariance matrix of the model is $R_j, j = 1, \ldots, r$, respectively. And R_1 is set to the normal measurement noise covariance matrix which is a white noise with a zero-mean Gaussian distribution of known statistical properties.

The model set is assumed to be M with r models. m_k is the effective model at time k. The dynamic system can be

expressed as:

$$\begin{cases} X_{k+1} = f(k, X_k) + G_k W_k \\ Z_k = h(k, X_k) + V_k \end{cases} \tag{13}$$

Initial Markov transition probability π_{ji} can be expressed as:

$$\pi_{ji} = P\left\{m_{k+1}^j | m_k^i\right\}, m_k^i, m_{k+1}^j \in M \tag{14}$$

The specific algorithm is as follows:

1) INITIALIZATION

At time k+1, the initial condition of the jth ($1 \le j \le r$) model filter is estimated by mixing the state of all filters from the previous time. Initial model transition probability $\mu_{k|k}^j$ is:

$$\mu_{k|k}^j = \frac{\pi_{ji}\mu_k^i}{\sum_{i=1}^r \pi_{ji}\mu_k^i} \tag{15}$$

μ_k^j is the probability of model i at time k.

Mixed state estimate $\hat{X}_k^j$ is:

$$\hat{X}_k^j = \sum_{i=1}^r \mu_{k|k}^j \hat{X}_k^i \tag{16}$$

Its estimated error covariance P_k^j is:

$$P_k^j = \sum_{i=1}^r \hat{\mu}_{k|k}^j \left[P_{k|k}^i + \left(\hat{X}_k^j - \hat{X}_{k|k}^i\right)\left(\hat{X}_k^j - \hat{X}_{k|k}^i\right)^T\right] \tag{17}$$

2) MATCHED FILTER

This step performs parallel filtering on each model. The algorithm uses an extended Kalman filter that is easy to implement in engineering as a matching model filter. For the jth model filter, the EKF algorithm is as follows:

$$\hat{X}_{k+1|k}^j = f(\hat{X}_{k|k}^j) \tag{18}$$

$$P_{k+1|k}^j = F_{k+1|k}^j P_{k|k}^j \left(F_{k+1|k}^j\right)^T + Q_k^j \tag{19}$$

$$e_{k+1}^j = Z_{k+1}^j - h(\hat{X}_{k+1|k}^j) \tag{20}$$

$$K_{k+1}^j = P_{k+1|k}^j \left(H_{k+1}^j\right)^T \times \left[H_{k+1}^j P_{k+1|k}^j \left(H_{k+1}^j\right)^T + R_{k+1}^j\right]^{-1} \tag{21}$$

$$\hat{X}_{k+1}^j = \hat{X}_{k+1|k}^j + K_{k+1}^j e_{k+1}^j \tag{22}$$

$$P_{k+1}^j = \left(I - K_{k+1}^j H_{k+1}^j\right) P_{k+1|k}^j \tag{23}$$

The state estimate $\hat{X}_{k+1}^j$ and the corresponding estimated covariance P_{k+1}^j are obtained by the above formula.

3) MODEL PROBABILITY UPDATE

The likelihood function Λ_{k+1}^j of model m_j can be simplified to:

$$\Lambda_{k+1}^j = N\left[(2\pi)^n |S_{k+1}^j|\right]^{-1/2} \times \exp\left\{-\frac{1}{2}\left(e_{k+1}^j\right)^T \left(S_{k+1}^j\right)^{-1} e_{k+1}^j\right\} \tag{24}$$

where n is the state dimension, the multi-model probability can be updated to

$$\mu_{k+1|k}^j = P\left\{m_{k+1}^j | Z_{k+1}^j\right\} = \frac{\Lambda_{k+1}^j \sum_{j=1}^r \pi_{ji}\mu_{k|k}^j}{\sum_{i=1}^r \left[\Lambda_{k+1}^j \sum_{j=1}^r \pi_{ji}\mu_{k|k}^j\right]} \tag{25}$$

Filtered innovation information e_{k+1}^j is calculated by (20). Its covariance is calculated as:

$$S_{k+1}^j = H_{k+1}^j P_{k+1|k} \left(H_{k+1}^j\right)^T + R_{k+1}^j \tag{26}$$

4) OUTPUT COMBINATION

The filtered state estimate is weighted by combining filter estimates based on each model.

$$\hat{X}_{k+1} = \sum_{j=1}^r \mu_{k+1|k}^j \hat{X}_{k+1}^j \tag{27}$$

$$P_{k+1} = \sum_{j=1}^r \mu_{k+1|k}^j \left[P_k + \left(\hat{X}_{k+1}^j - \hat{X}_{k+1}\right)\left(\hat{X}_{k+1}^j - \hat{X}_{k+1}\right)^T\right] \tag{28}$$

V. EXTREME LEARNING MACHINE

As shown in Fig.1 and Fig.2, we optimizes the new intelligent architecture based on ELM. When the GPS is available, IMM-EKF fuses GPS and de-noised INS data to correct INS position errors. And at the same time, INS position information and the output of IMM-EKF are used to train ELM. During GPS outages, ELM is used to predict the position errors of the INS.

Compared with the traditional single-hidden layer feedforward neural network (SLFNN), ELM is faster than traditional learning algorithms under the premise of ensuring learning accuracy. It is more suitable for GPS/INS integrated navigation to provide a fast, accurate and continuous navigation solution. The structural model of ELM is as follows:

With N samples (X_i, t_i), where $X_i = [x_{i1}, x_{i2}, \ldots, x_{in}] \in R^n$ and $t_i = [t_{i1}, t_{i2}, \ldots, t_{in}] \in R^m$, with L hidden nodes, the single-hidden layer neural network can be expressed as:

$$\sum_{i=1}^L \beta_i g\left(W_i \cdot X_j + b_i\right) = o_j, \quad j = 1, \ldots, N \tag{29}$$

where, $g(x)$ is the activation function, $W_i = [w_{i,1}, w_{i,2}, \ldots, w_{i,n}]^T$ is the input weight, β_i is the output weight, and

b_i is the hidden layer bias. $W_i \cdot X_j$ represents the inner product of the sum. The goal is to minimize the error of the output.

$$\sum_{j=1}^{N} \left\| o_j - t_j \right\| = 0 \tag{30}$$

It can be expressed mathematically as:

$$\sum_{i=1}^{L} \beta_i g\left(W_i \cdot X_j + b_i\right) = t_j, \quad j = 1, \ldots, N \tag{31}$$

Or it can be shown as:

$$H\beta = T \tag{32}$$

where, T is the target output, H is the hidden layer output matrix, and β is the output weight.

$$H\left(W_1, \ldots, W_L, b_1, \ldots, b_L, X_1, \ldots, X_L\right) = \begin{bmatrix} g\left(W_1 \cdot X_1 + b_1\right) & \cdots & g\left(W_L \cdot X_L + b_L\right) \\ \vdots & \cdots & \vdots \\ g\left(W_1 \cdot X_N + b_1\right) & \cdots & g\left(W_L \cdot X_N + b_L\right) \end{bmatrix}_{N \times L} \tag{33}$$

$$\beta = \begin{bmatrix} \beta_1^T \\ \vdots \\ \beta_L^T \end{bmatrix}_{L \times m} \quad T = \begin{bmatrix} T_1^T \\ \vdots \\ T_N^T \end{bmatrix}_{N \times m} \tag{34}$$

$\hat{W}_i$, $\hat{b}_i$ and $\hat{\beta}_i$ are expected to be obtained to train neural network.

$$\left\| H\left(\hat{W}_i, \hat{b}_i\right)\hat{\beta}_i - T \right\| = \min_{W,b,\beta} \left\| H\left(W_i, b_i\right)\beta_i - T \right\| \tag{35}$$

where $i = 1, \ldots, L$, this is equivalent to minimizing the loss function.

$$E = \sum_{j=1}^{N} \left(\sum_{i=1}^{L} \beta_i g\left(W_i \cdot X_j + b_i\right) - t_j \right)^2 \tag{36}$$

Some traditional algorithms based on the gradient descent method need to adjust all parameters during the iteration. ELM is a new SLFN algorithm. It will randomly generate input layers and the connection weight between the hidden layers and the threshold of the hidden layer neurons. It do not need be adjusted during the training process. It only needs to set the number of neurons in the hidden layer to obtain the unique optimal solution. Once the input weight and the hidden layer biases are randomly determined in the ELM algorithm, H is uniquely determined. Training SLFNN is equivalent to solving linear systems $H\beta = T$. And β can be determined.

$$\beta = H^* T \tag{37}$$

where, H^* is the Moore-Penrose generalized inverse of matrix H. More explanations about the ELM algorithm can be found in [28].

The GPS/INS algorithm based on ELM are as follows. The input parameters of the ELM algorithm consist of the training sample, activation function g(x) and the hidden nodes number. Note that according to Fig.1, the training input parameters are $<$ P_{INS}, Time $>$, and the training target outputs are filter outputs δP of IMM-EKF. Through detailed and repeated experiments, the number of hidden layer neurons and activation functions are determined through offline analysis of experimental data. According to the prediction mean square error results and training time corresponding to different numbers of nodes, the sigmoid function with 8 hidden nodes was used. In addition, the predicted output of ELM are $\delta P'$.

The ELM algorithm steps are as follows: (1) Input weight w_j and the bias b_j are initialized randomly for $j = 1, \ldots, N$. (2)Select the sigmoid function as the activation function of the hidden layer neurons and calculate the hidden layer output matrix H. (3)Calculate the output weight β using $\beta = H^*T$. H^* is the Moore-Penrose generalized inverse of matrix H. It can be calculated by the singular value decomposition (SVD).

TABLE 1. IMU specifications.

Specification	Gyroscope	Accelerometer
Dynamic range	±200°/sec	±4g
Bias stability	<10°/hr	<2mg
Resolution	<0.06°/sec	<0.6mg
Random walk	<4.5°/√hr	<1.0m/s/√hr

VI. EXPERIMENTAL

To verify the effectiveness of the proposed method, a low-cost MEMS-IMU, GPS receiver and navigation-grade SINS/GPS are installed at the center of the vehicle. Before each experiment, the inertial navigation system has completed initial alignment and infield calibration. After a calibration, the entire system is executed in the loosely coupled mode. The low-cost GPS receiver has a position measurement accuracy of 5m, a speed measurement accuracy of 0.05m/s, and the output frequency of 1Hz. The output frequency of the IMU is 200Hz. The technical specifications of the IMU are given in Table1. In addition, the navigation-grade SINS/GPS is used to provide position reference information in test 3. Its positioning accuracy is 0.01m when the GPS is available. When the GPS signal is interrupted for 10s, the positioning accuracy is 0.02m, and when the GPS signal is interrupted for 60s, the positioning accuracy is 0.23m.

Three road tests are implemented to verify the proposed method. Test 1 and 2 were selected for field measurements at the Taiyuan University of Technology. Test 1 mainly verifies the effectiveness of the wavelet de-noising algorithm based on EMD. We call this method EMD-WD. Test 2 mainly verifies the robustness of the IMM-EKF output results. Finally, Test 3 chooses to conduct field tests in downtown Taiyuan, Shanxi Province to evaluate the performance of the proposed method during real GPS outages. In the paper, the GPS outages are caused by high buildings, trees or bridges in urban

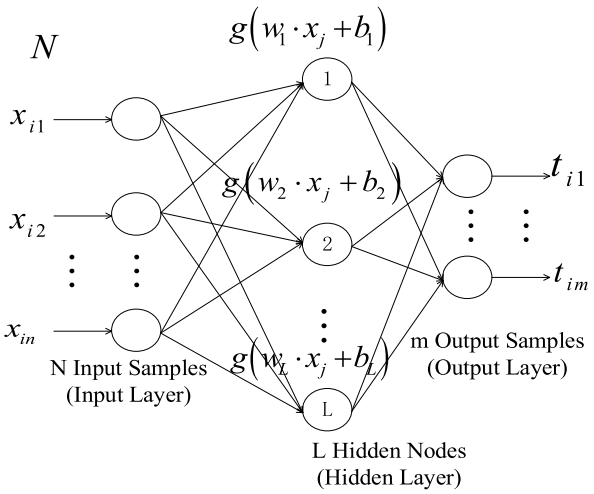

FIGURE 4. The structural model of ELM.

environments. By reading relevant articles and conducting repeated experiments, the GPS outages in urban environments are usually less than 40 seconds. In our tests, it is uniformly set to 60 seconds. When the outage is less than 60 seconds, it is artificially extended to 60 seconds.

A. TEST 1

Test 1 is mainly used to test the effectiveness of EMD-WD, and the experiments are conducted around the Taiyuan University of Technology. In the experiment, the number of accessible GPS satellites was more than four, and the number of barrier-free satellites was sufficient to meet the requirements of low-cost systems. Four GPS outages are simulated by manual removal of GPS observations during the experiments, and every outage lasts for 60 seconds. Some representative driving operations such as stop, turn and sudden acceleration/deceleration have been carried out. Several typical driving conditions, including straights, corners and intersections, as shown in Fig.5. In the following experiments, the coordinate system is established with the lower left corner of the trajectory map as the origin. And the position error refers to the horizontal Euclidean distance error between the estimated position and the corresponding reference value.

EMD implementation of data is a relatively time-consuming process. In order to realize the real-time solution, we uses a w-length sliding window. After the current data window is filtered, the data window continues to move forward for the next filtering. In order to balance the real-time performance and filtering performance of the algorithm, the length of the data window is selected as 2000.

In order to verify the validity of EMD-WD, this paper selects the raw data of the gyroscope Y-axis output as an example. The data results of other gyroscopes and accelerometers are similar to this result. Through experimental analysis, the EMD decomposition of the IMF components is determined to be 7 layers. The wavelet filter use wavelet function ''db6'' of 7-level wavelet decomposition with soft

FIGURE 5. Field test trajectory of test1.

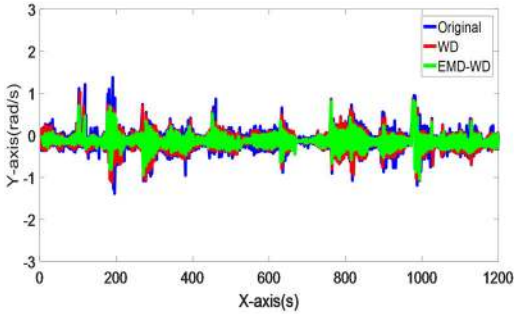

FIGURE 6. Comparison of Gyroscope Y-axis Output data.

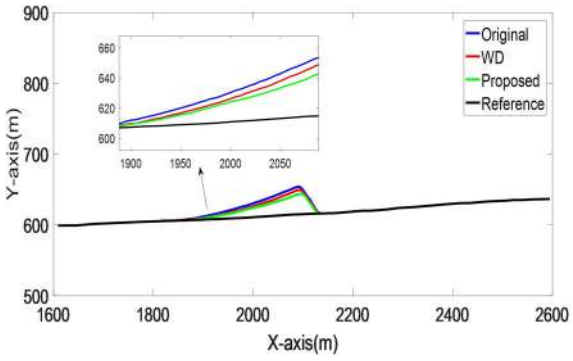

FIGURE 7. Positioning result in test 1 during GPS outage 2.

thresholding scheme based on Stein's Unbiased Risk Estimate (SURE) [29]. In addition, the wavelet de-noising (WD) algorithm is chosen for comparison

In Fig.6, the blue line represents the raw data of the gyroscope Y-axis output. The red line represents the gyroscope Y-axis data after WD. The green line represents the gyroscope Y-axis data after EMD-WD. It can be seen from the figure that EMD-WD can effectively eliminate noise interference in inertial navigation and improve navigation accuracy, which can provide reliable data for subsequent data fusion.

In order to show the effect of EMD-WD further, the GPS outage 2 and outage 3 in Test 1 are selected as examples. The gyroscope and accelerometer data are pre-processed, and then the mechanized equations are applied to obtain the INS position. Fig. 7 and Fig. 8 show the position errors of path 2 and path 3 during GPS outages. ''Reference'' represents the reference path. ''Original'' refers to the direct positioning of

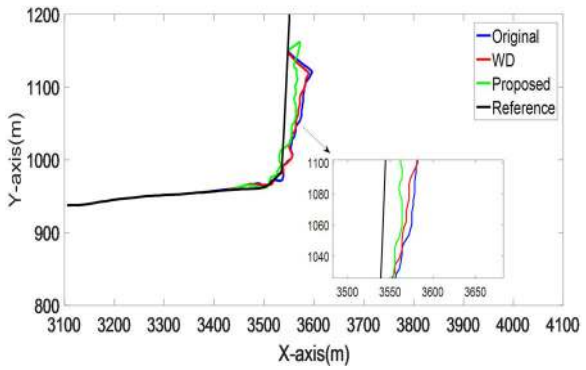

FIGURE 8. Positioning result in test 1 during GPS outage 3.

TABLE 2. Statistics of the position error during GPS outages in test 1.(Unit: m).

	Original		WD		Proposed	
	MAX	RMS	MAX	RMS	MAX	RMS
1	54.17	19.20	37.93	15.39	30.44	14.09
2	57.06	23.94	39.38	15.74	29.93	13.47
3	73.53	30.63	65.19	27.73	32.61	14.72
4	94.82	41.22	72.80	30.84	46.72	18.69

unprocessed inertial sensor data. ''WD'' refers to the positioning result of WD. ''Proposed'' refers to the positioning result of EMD-WD.

As shown in the Fig. 7, the outage 2 is a straight path. If the inertial navigation data is not processed, the error will increase rapidly. EMD-WD positioning performance is improved compared to WD.

The outage 3 is a turning path, and it can be clearly seen that the positioning performance of the proposed algorithm is greatly improved.

Table 2 is the comparison of position errors during GPS outages in Test 1. The maximum (MAX) value of the error and the root mean square (RMS) are used as the evaluation indicators.

It can be seen from the analysis of the above statistical results that the proposed pre-processing algorithm can effectively improve the positioning accuracy during GPS outages. During the four outages, the original method directly uses the raw output data of the MEMS INS. It has the worst positioning accuracy, and its MAX and RMS values are the largest. Compared with the original method, the positioning accuracy of WD has been improved, but the EMD-WD has the biggest improvement. Taking outage 2 as an example, the MAX of WD is 39.38m, and the RMS is 15.74m. For the original method, the corresponding values are 57.06m and 23.94m. The MAX of EMD-WD is 29.93m, the RMS is 13.47m. The main reason for these improvements is that the EMD-WD can effectively suppress the noise in the original data of inertial navigation. It can be seen that the EMD-WD can effectively improve the positioning performance. It not only provides more accurate information for later data fusion, but also provides more accurate training samples for ELM.

TABLE 3. Comparison of the positioning error results(Unit: m).

	EKF		IMM-EKF	
	MAX	RMS	MAX	RMS
1	18.12	10.12	15.32	8.55
2	20.94	11.61	16.80	9.15
3	17.35	9.03	14.16	7.39
4	18.54	10.46	15.28	8.92

B. TEST 2

In order to verify the robustness of the IMM-EKF, four 60-second road tests were conducted on the campus in Taiyuan University of Technology. Although the GPS can output positioning information in the actual measurement, there are many obstacles to reduce GPS performance in the campus. For example, multipath effects caused by high-rise buildings and trees or satellite instability will affect the positioning performance. This makes the measurement noise covariance in the Kalman filter algorithm change dynamically, which affects the positioning performance. In this paper, IMM-EKF is compared with the extended Kalman filter (EKF) algorithm. EKF has only one fixed initial measurement noise covariance. The IMM-EKF is set to three different measurement noise covariances.

The IMM-EKF algorithm is based on the Markov transformation matrix to achieve the change between the three models. The initial Markov transition probability π is as follows:

$$\pi_{ji} = \begin{cases} 0.95, & i = j \\ (1 - 0.95)/2, & i \neq j \end{cases} \quad (i, j = 1, 2, 3) \qquad (38)$$

In the experiment, the process noise covariance Q of IMM-EKF is considered to be constant, and the initial measurement noise covariance is set to $R = diag\left[10m \;\; 10m\right]^2$. The measurement noise matrices in the three parallel filters are set to R, 9R and 25R, respectively. As a comparison, the EKF process noise covariance is set to Q, and the initial measurement matrix is set to only R.

Table 3 shows the comparison of the positioning error results, and the MAX and RMS are selected as the evaluation indicators.

In order to evaluate the robustness of the IMM-EKF more clearly, additional noise is artificially inserted to change the measurement error of the GPS. The noise is modeled by a first-order Gauss-Markov process. After inserting additional

TABLE 4. Comparison of the positioning error results after noise insertion(Unit: m).

	EKF		IMM-EKF	
	MAX	RMS	MAX	RMS
1	26.73	13.05	17.09	9.26
2	27.16	14.08	18.54	9.72
3	23.59	11.96	15.50	8.74
4	28.02	13.71	16.19	10.16

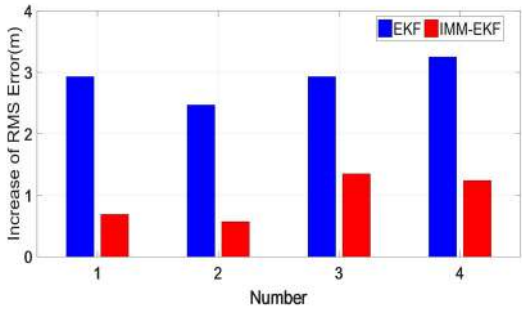

FIGURE 9. Increase of RMS error.

noise, the matrix R in the Kalman filter algorithm needs to be updated accordingly, which is not done in the general EKF. However, the IMM-EKF is set to three different measurement matrices. So it can switch between different models and accommodate the inserted noise better. Table 4 is a comparison of the positioning error results after noise insertion in the same path.

In order to display the robustness of the proposed IMM-EKF more intuitively, the increase of RMS error before and after noise insertion is shown in Fig.9.

In Fig.9, the increase of the RMS of IMM-EKF is significantly smaller than that of EKF after noise insertion. The increase of the RMS error of IMM-EKF is basically maintained within 1.5m. The error of EKF in the four tests increased by 2.93m, 2.47m, 2.93m, 3.25m, respectively. The RMS of IMM-EKF increased by 0.69m, 0.57m, 1.35m, and 1.24m, respectively. Therefore, the proposed IMM-EKF can adapt to the uncertain noise of GPS and improve the accuracy of target positioning, which provides more accurate training samples for ELM.

C. TEST 3

To evaluate the overall performance of the proposed method, real road experiments are conducted in Taiyuan city according to the experimental parameters settings in Test 1 and Test 2. The experimental route passes through real GPS outages caused by complex environments such as high-rise buildings, trees, bridges, and overpasses. When the outage is less than 60 seconds, it is artificially extended to

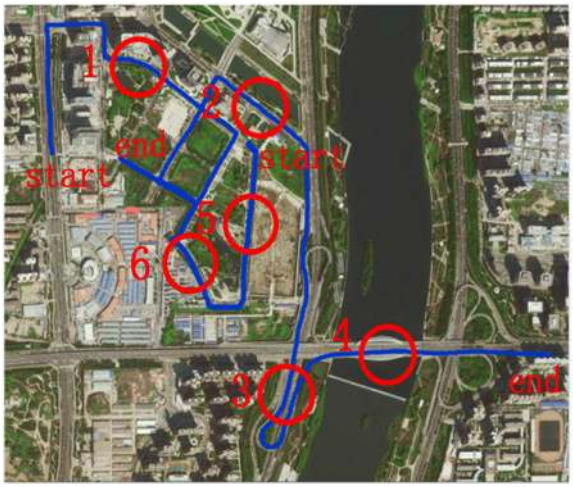

FIGURE 10. Field test trajectory of test 3.

60 seconds. In addition, a series of typical driving operations, such as vehicle lane change, acceleration and deceleration, are performed in the trajectory. The real trajectory is shown in the Fig. 10 and six representative outages were selected. When the GPS is available,EMD-WD/IMM-EKF is used to correct INS position errors. At the same time, INS position information and the output of IMM-EKF are used to train ELM. During GPS outages, EMD/ELM is used to predict the output of IMM-EKF, which is the INS position error. In order to highlight the effectiveness of the proposed EMD-WD/IMM-EKF/ELM method, ELM/IMM-EKF, RBF/EKF and EKF were selected for comparison.

EKF method. This method uses EKF to achieve the fusion of INS and GPS, and then output positioning information when the GPS is available. The positioning information is separately output by the INS during GPS outages. RBF/EKF method. RBF/EKF is the most commonly used reference algorithm in this research area [17], [18], [13]. During GPS outages, the method uses RBF to predict and correct INS errors. IMM-EKF/ELM method. Compared with the method RBF/EKF, the improvement of the method is that the IMM-EKF is used to improve the accuracy of the Kalman filter output, and the ELM is used to replace RBF. These methods mentioned above all use the data directly output by the MEMS-INS. Table 5 shows the quantitative comparison of MAX and RMS of the position error during six GPS outages.

The positioning error during GPS outages 1 in test 3 is shown in Fig. 11. The vehicle travels along an approximate arc during GPS outage 1. It can be clearly seen from the figure that the proposed method has higher performance compared to EKF and RBF/EKF. Comparing the green and purple lines in the graph, it can be concluded that additional precision improvements can be achieved with the EMD-WD. It can be seen from the table that the MAX of EKF reaches 60.02m, which has seriously affected the positioning performance. The MAX of RBF/EKF is 41.14m. The MAX of the proposed algorithm is only 17.12m. Compared with

TABLE 5. Comparison of the position errors during GPS outages of test 3. (Unit: m).

	EKF		RBF/EKF		ELM/IMM-EKF		PROPOSED	
	MAX	RMS	MAX	RMS	MAX	RMS	MAX	RMS
1	60.20	27.95	41.41	20.54	34.91	16.53	17.12	7.96
2	61.09	28.61	49.10	22.34	43.75	18.02	24.30	11.54
3	71.19	33.79	58.69	26.07	39.91	17.37	15.99	8.79
4	58.73	26.32	43.12	18.04	38.40	16.07	18.92	9.94
5	64.58	28.9	55.36	22.35	40.03	18.28	27.22	11.84
6	60.97	25.83	47.88	22.17	38.09	16.57	19.35	8.89

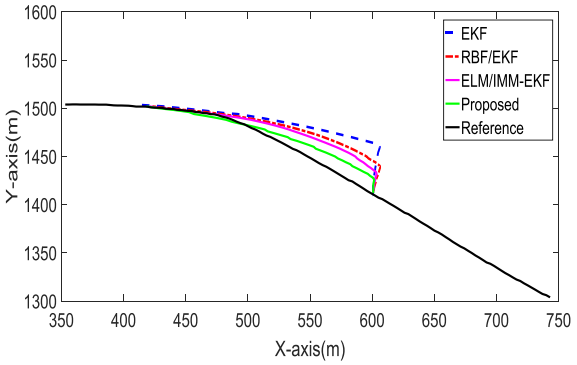

FIGURE 11. Performance during GPS outage 1 in test 3.

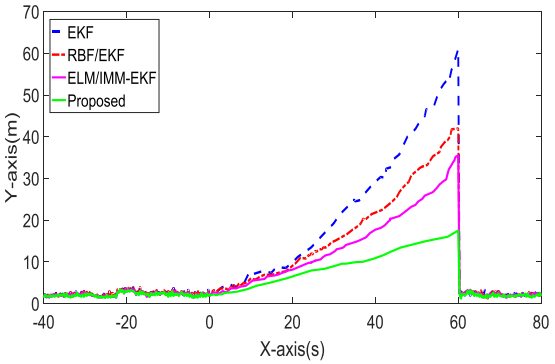

FIGURE 12. The curve of positioning residuals.

the EKF without any processing, the MAX reduces 43.08m and improves 71.56%. Compared to the ELM/IMM-EKF, the MAX reduces 17.79m and RMS reduces 8.57m.

The GPS outage 1 in test 3 is taken as an example to provide the positioning residual curve for distinguish the positioning errors of different algorithms. The results of other outages in test 3 are similar to this result. Fig. 12 shows the residual curve before and after GPS outage 1. The negative sign on the X axis indicates that this time occurred before the GPS outage. −40s refers to 40 seconds before the interruption. As shown in Fig. 12, the curve corresponding to 0s-60s is the residual curve during GPS outage. The curve corresponding to the rest of the time on X axis represents the positioning curve when GPS is not interrupted. During GPS outage, the position error of the proposed algorithm is significantly reduced.

The vehicle travels in a straight line during GPS outage 2. As shown in Fig. 13, compared with EKF, the other three methods have achieved good results. The

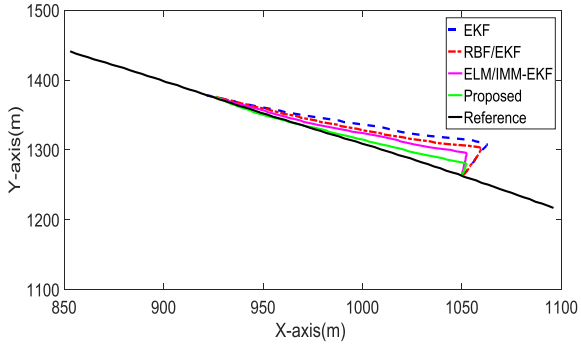

FIGURE 13. Performance during GPS outage 2 in test 3.

MAX of ELM/IMM-EKF is 17.34m less than the EKF, which gives the validity of the ELM/IMM-EKF method. After further pre-processing the inertial navigation data, its MAX reduces 19.45m compared to ELM/IMM-EKF. It is further explained that the pre-processing algorithm EMD-WD can effectively improve the positioning accuracy.

TABLE 6. Improvement result for the proposed method.

		Proposed method Against EKF		Proposed method Against RBF/EKF		Proposed method Against ELM/IMM-EKF	
		MAX	RMS	MAX	RMS	MAX	RMS
1	Error reduction	43.08	19.99	24.29	12.58	17.79	8.57
	Improvement %	71.56	71.52	58.66	61.25	50.96	51.85
2	Error reduction	36.79	17.07	24.80	10.70	19.45	6.48
	Improvement %	60.22	59.44	50.51	47.90	44.46	35.96
3	Error reduction	55.20	25.00	42.70	17.28	23.92	8.58
	Improvement %	77.54	73.99	72.76	66.28	59.93	49.40
4	Error reduction	39.81	16.38	24.20	8.10	19.48	6.13
	Improvement %	67.78	62.23	56.12	44.90	50.73	38.15
5	Error reduction	37.36	17.06	28.14	10.51	12.81	6.64
	Improvement %	57.85	59.03	50.83	47.02	47.06	56.08
6	Error reduction	41.62	16.94	28.53	13.28	18.74	7.68
	Improvement %	68.26	65.58	59.59	59.90	49.20	46.35

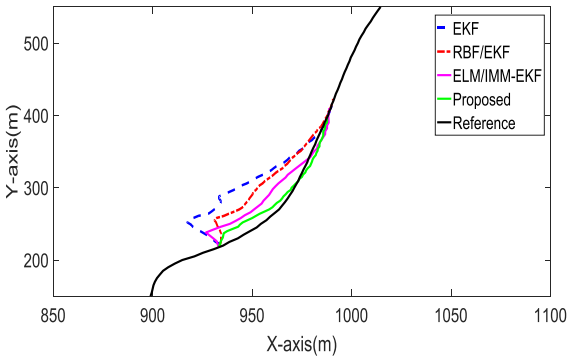

FIGURE 14. Performance during GPS outage 3 in test 3.

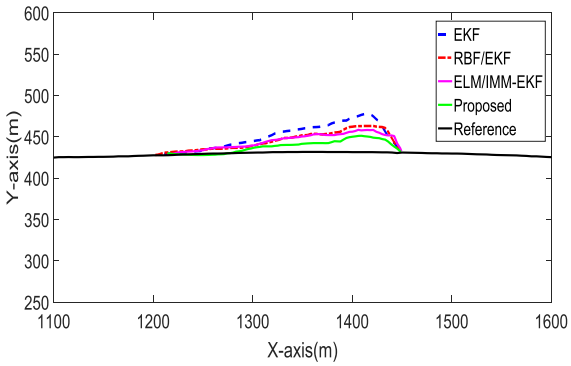

FIGURE 15. Performance during GPS outage 4 in test 3.

Compared with EKF, RBF/EKF, ELM/IMM-EKF and the proposed algorithm improves by 59.44%, 47.90%, and 35.96%, respectively.

The vehicle passes through the overpass during GPS outage 3. As shown in Fig. 14, it can be clearly seen from the figure that the positioning performance of EKF is the worst. Compared with the other three methods, the proposed algorithm achieves higher precision. Both the MAX and RMS of the proposed algorithm are reduced. The MAX and RMS of the RBF/EKF are 58.69m and 26.07m respectively. The proposed algorithm is 15.99m and 8.79m respectively.

The vehicle passes through the bridge during GPS outage 4. Fig. 15 is the positioning result during GPS outage 4. It can be clearly seen from the figure that the positioning performance of the EKF is the worst, and other methods have a certain improvement. The error of the three methods is slowly accumulating, but the proposed algorithm tends to be flat. Its MAX and RMS are the smallest, 18.92m and 9.94m, respectively.

The vehicle travels in a straight line during GPS outage 5. As shown in the Fig. 16, it can be seen from the figure that compared with EKF method, the other three methods have achieved better results. The MAX of the proposed algorithm is 27.22m, the MAX of EKF is 64.58m, the MAX of RBF/EKF is 55.36m, and the MAX of ELM/IMM-EKF is 40.03m. The MAX of the proposed method is 50.83% less than RBF/EKF, which proves that EMD-WD/IMM-EKF/ELM is more effective than RBF/EKF. Moreover,

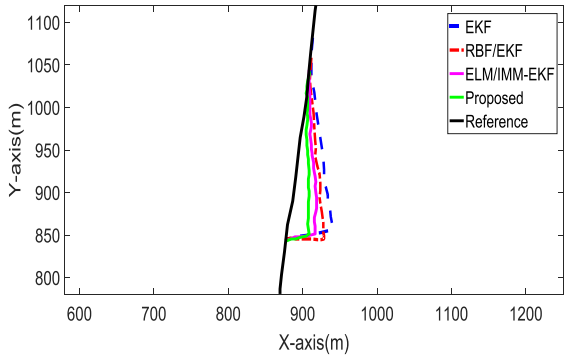

FIGURE 16. Performance during GPS outage 5 in test 3.

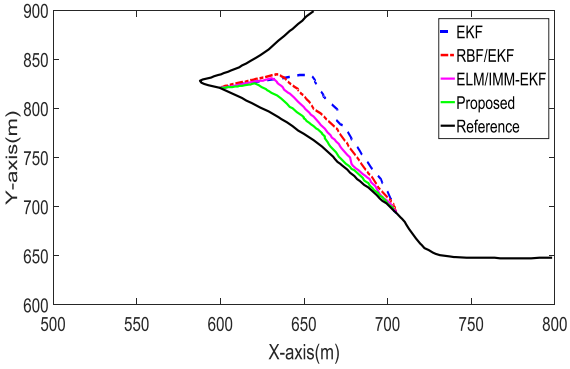

FIGURE 17. Performance during GPS outage 6 in test 3.

by comparing the positioning results of EMD-WD/IMM-EKF/ELM and ELM/IMM-EKF it can further verified the effectiveness of EMD-WD.

The vehicle passes through the curved street during GPS outage 6. Fig. 17 is the positioning result during GPS outage 6. The MAX of EMD-WD/IMM-EKF/ELM is 19.35m, and the MAX of EKF, RBF/EKF and ELM/IMM- EKF are 60.97m, 47.88m, and 38.09m, respectively. The MAX decreased by 68.26%, 59.59%, and 49.20%, respectively.

It can be seen from Table 5 and Fig.11 to Fig. 17 that the proposed method can achieve accurate and reliable positioning regardless of the change of the external environment. The main reason for the improvement is because not only ELM has more learning ability, but also two processing methods were used to improve the accuracy of the ELM training samples. EMD-WD effectively suppresses random noise in inertial data. IMM-EKF improves the output of Kalman filter. They improve the effectiveness of modeling and achieve more effective compensation for INS position error. In order to quantify the comparison between the proposed method and the other three methods, table 6 compares the MAX and RMS error reduction between the proposed method and the other three methods, and the performance improvement against the other three methods.

VII. CONCLUSION

The experimental parameters are analyzed offline and the hybrid fusion algorithm is real-time. The simulation experiment uses MATLAB 2016 software. Multiple simulation experiments were performed on a laptop computer (8G, Intel Core i7-3612QM CPU @ 2.10GHz 2.10GHz), and the corresponding program running time was statistically analyzed. In terms of real-time evaluation, with the above-mentioned software and hardware configuration, for the algorithm proposed in this paper, the statistical results show that the entire system takes 0.018951s to complete a recursion. The frequency of INS strapdown solution is set to 20Hz and the frequency of GPS to correct INS is set to 1Hz. Therefore, the proposed method meets the real-time requirements of combined positioning systems. We can claim the effectiveness of the algorithm proposed in this paper. However, when different equipment and experimental environments are used, we do not claim that the parameters of this article are set to the best combination.

This paper mainly studies the low-cost, high-reliability MEMS INS/GPS information fusion algorithm, and the proposed method can achieve accurate positioning during GPS outages. Based on the original wavelet threshold de-noising, a new wavelet threshold de-noising based on EMD is proposed, which is called EMD-WD. And the interactive multi-model algorithm is introduced into EKF, which is IMM-EKF. Finally, this paper optimizes the new intelligent architecture based on ELM. During GPS outages, we also provide a fast, accurate and continuous navigation solution. When the GPS is available, IMM-EKF fuses GPS and de-noised INS data to correct INS position errors. At the same time, INS position information and the outputs of IMM-EKF are used to train ELM. During GPS outages, ELM is used to predict the INS position errors. The performance of the proposed integrated positioning method is very competitive for using low cost MEMS INS/GPS. This method can be used in all environments, including frequent GPS outages in urban environments. This method has been verified in the road tests, and the results show the effectiveness of the proposed method.

REFERENCES

[1] Y. Kim, J. An, and J. Lee, "Robust navigational system for a transporter using GPS/INS fusion," *IEEE Trans. Ind. Electron.*, vol. 65, no. 4, pp. 3346–3354, Apr. 2017.

[2] T.-H. Chang, L.-S. Wang, and F.-R. Chang, "A solution to the ill-conditioned GPS positioning problem in an urban environment," *IEEE Trans. Intell. Transp. Syst.*, vol. 10, no. 1, pp. 135–145, Mar. 2009.

[3] M. M. Atia, S. Liu, H. Nematallah, T. B. Karamat, and A. Noureldin, "Integrated indoor navigation system for ground vehicles with automatic 3-D alignment and position initialization," *IEEE Trans. Veh. Technol.*, vol. 64, no. 4, pp. 1279–1292, Apr. 2015.

[4] P. Liu, B. Wang, Z. Deng, and M. Fu, "INS/DVL/PS tightly coupled underwater navigation method with limited DVL measurements," *IEEE Sensors J.*, vol. 18, no. 7, pp. 2994–3002, Apr. 2018.

[5] Y. Yao, X. Xu, C. Zhu, and C.-Y. Chan, "A hybrid fusion algorithm for GPS/INS integration during GPS outages," *Measurement*, vol. 103, pp. 42–51, Jun. 2017.

[6] J. Li, N. Song, G. Yang, M. Li, and Q. Cai, "Improving positioning accuracy of vehicular navigation system during GPS outages utilizing ensemble learning algorithm," *Inf. Fusion*, vol. 35, pp. 1–10, May 2017.

[7] R. Van der Merwe and E. A. Wan, "The square-root unscented Kalman filter for state and parameter-estimation," in *Proc. IEEE Int. Conf. Acoust., Speech, Signal Process.*, May 2002, pp. 3461–3464.

[8] H. Han, J. Wang, and M. Du, "GPS/BDS/INS tightly coupled integration accuracy improvement using an improved adaptive interacting multiple model with classified measurement update," *Chin. J. Aeronaut.*, vol. 31, no. 3, pp. 556–566, Mar. 2018.
[9] Q. Xu, X. Li, and C.-Y. Chan, "Enhancing localization accuracy of MEMS-INS/GPS/In-Vehicle sensors integration during GPS outages," *IEEE Trans. Instrum. Meas.*, vol. 67, no. 8, pp. 1966–1978, Aug. 2018.
[10] M. Quddus and S. Washington, "Shortest path and vehicle trajectory aided map-matching for low frequency GPS data," *Transp. Res. C, Emerg. Technol.*, vol. 55, pp. 328–339, Jun. 2015.
[11] B. Liu, X. Zhan, and M. Liu, "GNSS/MEMS IMU ultra-tightly integrated navigation system based on dual-loop NCO control method and cascaded channel filters," *IET Radar, Sonar Navigat.*, vol. 12, no. 11, pp. 1241–1250, Nov. 2018.
[12] X. Li, W. Chen, C. Chan, B. Li, and X. Song, "Multi-sensor fusion methodology for enhanced land vehicle positioning," *Inf. Fusion*, vol. 46, pp. 51–62, Mar. 2018.
[13] S. Adusumilli, D. Bhatt, H. Wang, P. Bhattacharya, and V. Devabhaktuni, "A low-cost INS/GPS integration methodology based on random forest regression," *Expert Syst. Appl.*, vol. 40, no. 11, pp. 4653–4659, Sep. 2013.
[14] Y. Zhang, C. Shen, J. Tang, and J. Liu, "Hybrid algorithm based on MDF-CKF and RF for GPS/INS system during GPS outages (April 2018)," *IEEE Access*, vol. 6, pp. 35343–35354, 2018.
[15] M. Malleswaran, V. Vaidehi, and N. Sivasankari, "A novel approach to the integration of GPS and INS using recurrent neural networks with evolutionary optimization techniques," *Aerosp. Sci. Technol.*, vol. 32, no. 1, pp. 169–179, Jan. 2014.
[16] P. Aggarwal, D. Bhatt, V. Devabhaktuni, and P. Bhattacharya, "Dempster Shafer neural network algorithm for land vehicle navigation application," *Inf. Sci.*, vol. 253, pp. 26–33, Dec. 2013.
[17] X. Lei and J. Li "An adaptive navigation method for a small unmanned aerial rotorcraft under complex environment," *Measurement*, vol. 46, no. 10, pp. 4166–4171, 2013.
[18] D. Bhatt, P. Aggarwal, V. Devabhaktuni, and P. Bhattacharya, "A novel hybrid fusion algorithm to bridge the period of GPS outages using low-cost INS," *Expert Syst. Appl.*, vol. 41, no. 5, pp. 2166–2173, Apr. 2014.
[19] A. Noureldin, A. El-Shafie, and M. Bayoumi, "GPS/INS integration utilizing dynamic neural networks for vehicular navigation," *Inf. Fusion*, vol. 12, no. 1, pp. 48–57, Jan. 2011.
[20] X. Chen, C. Shen, W.-B. Zhang, M. Tomizuka, Y. Xu, and K. Chiu, "Novel hybrid of strong tracking Kalman filter and wavelet neural network for GPS/INS during GPS outages," *Measurement*, vol. 46, no. 10, pp. 3847–3854, Dec. 2013.
[21] C. Stiller, F. P. León, and M. Kruse, "Information fusion for automotive applications—An overview," *Inf. Fusion*, vol. 12, no. 4, pp. 244–252, 2011.
[22] L. Wang and S. Li, "Enhanced multi-sensor data fusion methodology based on multiple model estimation for integrated navigation system," *Int. J. Control, Autom. Syst.*, vol. 16, no. 1, pp. 295–305, Feb. 2018.
[23] M. R. Kaloop and H. Li, "Multi input–single output models identification of tower bridge movements using GPS monitoring system," *Measurement*, vol. 47, pp. 531–539, Jan. 2014.
[24] R. P. Shao, J. M. Cao, and Y. L. Li, "Gear fault pattern identification and diagnosis using time-frequency analysis and wavelet threshold de-noising based on EMD," *J. Vib. Shock*, vol. 31, no. 8, pp. 96–101 and 106, 2012.
[25] L. I. Yue, J. L. Peng, H.-B. Lin, and M. A. Hai-Tao, "Study of the influence of transition IMF on EMD do-noising and the improved algorithm," *Chin. J. Geophys.*, vol. 56, no. 2, pp. 626–634, 2013.
[26] M. Ushaq, F. J. Cheng, and J. Ali, "An adaptive & fault tolerant sins/gps integrated navigation scheme robustified against slowly growing errors in GPS updates," *Appl. Mech. Mater.*, vol. 390, pp. 500–505, Aug. 2013.
[27] E. S. Abdolkarimi, G. Abaei, and M. R. Mosavi, "A wavelet-extreme learning machine for low-cost INS/GPS navigation system in high-speed applications," *GPS Solutions*, vol. 22, no. 1, p. 15, Jan. 2018.
[28] G. B. Huang, Q. Y. Zhu, and C. K. Siew, "Extreme learning machine: Theory and applications," *Neurocomputing*, vol. 70, no. 1, pp. 489–501, 2006.
[29] A. Quinchia, G. Falco, E. Falletti, F. Dovis, and C. Ferrer, "A comparison between different error modeling of MEMS applied to GPS/INS integrated systems," *Sensors*, vol. 13, no. 8, pp. 9549–9588, 2013.

DENGAO LI was born in Shanxi, China, in 1971. He is currently a Professor with the Taiyuan University of Technology. He has worked on the projects funded by the National "863" Project and the National Nature Funds. His research interests include medical signal processing, satellite signal processing, and powerless sensing. He is the Chair of the ACM Taiyuan Chapter, the Director of the Communication Institute of Shanxi, and the Director of the Internet Association of Shanxi.

XUAN JIA was born in Shanxi, China, in 1993. He is currently pursuing the M.S. degree with the Taiyuan University of Technology. His research interests include satellite signal processing and GPS/INS integrated navigation systems.

JUMIN ZHAO was born in Shanxi, China, in 1976. She is currently a Professor with the Taiyuan University of Technology. She has worked on the projects funded by the National "863" Project and the National Nature Funds. Her research interests include cyber-physical systems and weak signal processing. She is a Senior Member of the CIE, a member of the CIE-YoSC, the Deputy Secretary-General of the ACM Taiyuan Chapter, and a Committee Member of the CCF.